

Metal-insulator transition in $\text{Al}_x\text{Ga}_{1-x}\text{As}/\text{GaAs}$ heterostructures with large spacer width

A. Gold*

Department of Physics, Massachusetts Institute of Technology, Cambridge, Massachusetts 02139

(Received 19 June 1989; revised manuscript received 21 March 1991)

Analytical results are presented for the mobility of a two-dimensional electron gas in a heterostructure with a thick spacer layer α . Due to multiple-scattering effects a metal-insulator transition occurs at a critical electron density $N_c = N_i^{1/2}/(4\pi^{1/2}\alpha)$ (N_i is the impurity density). The transport mean free path $l^{(t)}$ (calculated in Born approximation) at the metal-insulator transition is $l_c^{(t)} = 2\alpha$. A localization criterion in terms of the renormalized single-particle mean free path $l^{(sr)}$ is presented: $k_{Fc} l_c^{(sr)} = (\frac{1}{2})^{1/2}$ (k_{Fc} is the Fermi wave number at the critical density). I compare the theoretical results with recent experimental results found in $\text{Al}_x\text{Ga}_{1-x}\text{As}/\text{GaAs}$ heterostructures with large spacer width: $1200 < \alpha < 2800 \text{ \AA}$. Remote impurity doping and homogeneous background doping are considered. The only fitting parameter used for the theoretical results is the background doping density $N_B = 6 \times 10^{13} \text{ cm}^{-3}$. My theory is in fair agreement with the experimental results.

I. INTRODUCTION

The scaling theory for noninteracting electron gases predicted for two-dimensional systems a localized phase for arbitrarily weak disorder.¹ A complete theory for a disordered interacting electron gas is not yet available, for a review see Ref. 2. Obviously, according to this prediction, a two-dimensional metal with finite conductivity does not exist (for temperature zero).

However, in transport measurements of the two-dimensional electron gas in $\text{Al}_x\text{Ga}_{1-x}\text{As}/\text{GaAs}$ heterostructures the mobility record has been improved every year in the past few years.³⁻⁵ The best reported mobility at this time is $1.1 \times 10^7 \text{ cm}^2/\text{V s}$.⁵ There seems to exist a growing discrepancy between experiments³⁻⁵ and theory.¹ In this paper we will argue that this discrepancy disappears if one accepts the concept of a metal-insulator transition (MIT) in $\text{Al}_x\text{Ga}_{1-x}\text{As}/\text{GaAs}$ heterostructures. Whether this MIT is similar to a transition from a weakly localized system to a strongly localized system remains an open question.

Strong deviations of the mobility from the lowest-order result have recently been found in $\text{Al}_x\text{Ga}_{1-x}\text{As}/\text{GaAs}$ heterostructures with large spacers α ($\alpha \simeq 500 \text{ \AA}$).⁶ The anomalies occur for $2 \times 10^{10} < N < 4 \times 10^{10} \text{ cm}^{-2}$ and an electron-density threshold for a finite mobility was reported. Evidence for a metal-insulator transition in two-dimensional systems have been found in silicon metal-oxide-semiconductor structures (for a review, see Ref. 7) and $\text{In}_{1-x}\text{Ga}_x\text{As}$ quantum wells.⁸ Therefore, the authors of Ref. 9 argued to neglect the weak-localization corrections and formulated a theory for the MIT in two dimensions for disordered electron systems. Experiments on the mobility of silicon metal-oxide-semiconductor structures have been explained with this theory.

Transport properties of $\text{Al}_x\text{Ga}_{1-x}\text{As}/\text{GaAs}$ heterostructures are presently studied in great detail. For a recent review, see Ref. 10. The results of Ref. 6 have been interpreted quantitatively¹¹ as transport near the MIT

within the multiple-scattering approach of Ref. 9. Efros¹² argued for transport near the percolation threshold.

In this paper we show that the multiple-scattering approach and the percolation theory give essentially the same criterion for the metal-insulator transition point. Analytical results for the mobility and the transition point within the multiple-scattering theory are derived. We use the analytical results to analyze recent experiments on the mobility of $\text{Al}_x\text{Ga}_{1-x}\text{As}/\text{GaAs}$ heterostructures with ultralarge spacers ($1200 < \alpha < 2800 \text{ \AA}$) (Ref. 13) at low electron densities: $4 \times 10^9 < N < 1 \times 10^{11} \text{ cm}^{-2}$. The results of my theory compare favorably with the experiments¹³ and indicate that the theory describes the transport properties of disordered two-dimensional systems at low temperatures.

The paper is organized as follows. In Sec. II the model and the theory is described. The analytical results are given in Sec. III. In Sec. IV I compare the theory with recent experimental results. The discussion is in Sec. V. I conclude in Sec. VI.

II. MODEL AND THEORY

A. Model

The model for remote impurity doping is characterized by a sheet of randomly distributed impurities (with impurity density N_i) separated from the ideally two-dimensional electron gas (with electron density N) by a spacer of width α . The Fourier transform of the random potential $\langle |U(q)|^2 \rangle$ is given by

$$\langle |U(q)|^2 \rangle = N_i \left[\frac{2\pi e^2}{\epsilon_L q} \right]^2 e^{-2q\alpha}. \quad (1)$$

ϵ_L is the dielectric constant of the background. In general, the screening function $\epsilon(q)$ of the interacting electron gas is expressed in terms of the polarizability $X^0(q)$ of the free-electron gas and the electron-electron interaction potential.⁷ The parameters (see later) of the theory

are defined as q integrals over the screened random potential. For large spacer width, $4k_F\alpha \gg 1$, I use X^0 ($q \leq 2k_F$) = ρ_F .⁷ k_F is the Fermi wave number and ρ_F is the density of states. For the ideally two-dimensional electron gas the electron-electron interaction potential is $V(q) = 2\pi e^2 / \epsilon_L q$ and the screening function is given by

$$\epsilon(q) = 1 + q_s / q . \quad (2a)$$

q_s is the screening wave number, given by the effective Bohr radius a^* ($a^* = \epsilon_L \hbar^2 / m^* e^2$) and the valley degeneracy g_v : $q_s a^* = 2g_v$. m^* is the effective electron mass. For $2\alpha q_s = 4g_v \alpha / a^* \gg 1$ I simply use

$$\epsilon(q) = q_s / q . \quad (2b)$$

This approximation has been discussed in Ref. 14 and was later applied in Ref. 12. With Eq. (2b) I get for the screened random potential $\langle |U(q)|^2 \rangle / \epsilon(q)^2 \simeq N_i e^{-2q\alpha}$. This screened potential represents a long-range random potential with reduced backscattering.

I assume an ideally two-dimensional electron gas in a plane and neglected the extension of the electron gas perpendicular to the plane. This extension is characterized by the parameter $1/b$, see Eq. (3.30) of Ref. 7. b is of order $1/a^*$. For $ab \gg 3$ one can neglect the extension of the electron gas perpendicular to the plane.

B. Theory

In the multiple-scattering theory^{15,16} for the conductivity of a disordered noninteracting electron gas at zero temperature the crossed diagrams² are neglected. However, the ladder diagrams are taken into account. For a disordered interacting electron gas the interaction effects are treated in the random-phase approximation.^{9,17} The theory describes a transition from a metallic phase (for weak disorder) to an insulating phase (for strong disorder) due to multiple-scattering effects. The conductivity for weak disorder is given within the Born approximation (σ_0) and the conductivity near the transition point to an insulator is given as a scaling law (σ_c). In experiments on two-dimensional systems the scaling law has not yet been identified.⁶⁻⁸ It would be highly desirable to get more experimental results on the behavior of the conductivity near the metal-insulator transition. It is one goal of the present paper to supply information on the relevant doping parameters for an optimal design of samples for a study of strong disorder effects in two-dimensional electron systems.

The important parameter A of the multiple-scattering theory for an interacting electron gas in two dimensions^{9,14,17} is defined as

$$A = \frac{1}{4\pi N^2} \int_0^\infty dq q \frac{\langle |U(q)|^2 \rangle}{\epsilon(q)^2} X^0(q)^2 . \quad (3)$$

The parameter A defines the metal-insulator transition point. For $A < 1$ the system is metallic and for $A > 1$ the system has the transport properties of an insulator.^{15,16} The transition occurs at $A = 1$.

A generalized hydrodynamic approximation was used to derive the scaling law for disordered noninteracting

electrons within the multiple-scattering theory.^{18,19} The importance of the crossed diagrams decreases (compared to the ladder diagrams) if the potential becomes long ranged.¹⁹ It was pointed out in Ref. 19 that for long-ranged random potentials a percolation picture is applicable to the metal-insulator transition. A similar approximation as in Refs. 18 and 19 gives for the disordered interacting electron gas

$$\sigma(N) = \sigma_0(N)(1 - A) \quad (\text{for } A \sim 1) . \quad (4)$$

$\sigma_0(N)$ is the conductivity in Born approximation. Equation (4) has the correct limit $\sigma(N) \simeq \sigma_0(N)$ for weak disorder ($A \ll 1$) and is also a good approximation to the solution of the self-consistent equation.

III. ANALYTICAL RESULTS

In this section I present the analytical results for the metal-insulator transition (Sec. III A) and the conductivity (Sec. III B) for remote doping and large spacer width. I calculate the mean free path at the transition point and discuss the Joffe-Regel criterion (Sec. III C). Effects of a disorder-induced modification of the density of states are derived (Sec. III D). Results for various doping structures are discussed (Sec. III E).

A. The critical electron concentration

With $X^0(q) = \rho_F$ and Eqs. (1), (2b), and (3) I get

$$A = \frac{N_i}{16\pi N N \alpha^2} . \quad (5)$$

With Eq. (5) I derive the critical electron density N_c for the metal-insulator transition

$$N_c = \frac{N_i^{1/2}}{4\pi^{1/2}\alpha} = 0.141 N_i^{1/2} / \alpha . \quad (6)$$

The experimental results on the spacer width dependence of the threshold in $\text{Al}_x\text{Ga}_{1-x}\text{As}/\text{GaAs}$ heterostructures⁶ are in good agreement with Eq. (6).¹¹ Efros¹² found

$$N_c = \beta N_i^{1/2} / \alpha \quad (7)$$

with $\beta \sim 0.1$. However, it is not clear how Efros estimated β . I conclude that the multiple-scattering approach gives for N_c essentially the same result as the percolation approach.

B. The conductivity

For $N \gg N_c$ multiple-scattering effects are negligible and the conductivity can be calculated in Born approximation. With Eq. (2b) one gets^{16,20,21}

$$\sigma_0(N) = 2g_v^2 \frac{e^2}{h} \frac{N}{N_i} (2k_F \alpha)^3 \quad (\text{for } N \gg N_c) . \quad (8)$$

With Eqs. (4), (5), and (8) I find for the conductivity near the metal-insulator transition

$$\sigma_c(N) = 2\sigma_0(N_c) \left[\frac{N - N_c}{N_c} \right]^1 \quad (\text{for } N \simeq N_c) , \quad (9a)$$

with

$$\sigma_0(N_c) = g_v \frac{e^2}{h} 2k_{Fc} \alpha. \quad (9b)$$

Efros¹² proposed, without derivation,

$$\sigma_c(N) = \beta \sigma_0(N_c) \left[\frac{N - N_c}{N_c} \right]^t \quad (\text{for } N \sim N_c). \quad (10)$$

The critical exponent for percolation in two dimensions is $t = 1.2$ (for a review, see Ref. 22) and β was unspecified in Ref. 12. Efros cited Ref. 23 for the derivation of Eq. (10). However, I could not find Eq. (10) with the prefactor $\sigma_0(N_c)$ in Ref. 23. In addition to the critical exponent the results within the percolation approach [Eq. (10)] and within the multiple-scattering approach [Eq. (9)] are very similar: The scale of the conductivity is given by $\sigma_0(N_c)$.¹⁶

In the original formulation of the multiple-scattering theory^{9,15,16} the critical exponent was given as $t = \frac{1}{2}$. In this formulation one derives a scaling law as given in Eq. (10) with $t = \frac{1}{2}$, $\beta = (\frac{4}{3})^{1/2}$, and with the correct scale of the conductivity: $\sigma_0(N_c)$.

By comparing Eqs. (9) and (10) I mention the following: The range of the scaling laws is small:¹⁷ $N/N_c - 1 \equiv \epsilon < 0.1$. With Eqs. (4), (5), and (8) one gets

$$\sigma_c(\epsilon \ll 1) = 2\sigma_0(N_c) \epsilon [1 + \epsilon + \epsilon^2/8 + O(\epsilon^3)]. \quad (11)$$

This scaling law has an accuracy of 10% for $\epsilon \approx 0.1$. Experimentally the scaling law has not yet been observed. For the experiment on the threshold transport,⁶ the condition $\epsilon < 0.1$ would imply to measure the mobility for $\mu < 10^4 \text{ cm}^2/\text{Vs}$. It will be probably very difficult to induce such small density variations that the critical exponent can be determined.

The multiple-scattering approach does not focus on the exact calculation of the critical exponent t . It is rather a powerful method for the calculation of the conductivity in the full density range including the metal-insulator transition point. This has been demonstrated for silicon metal-oxide-semiconductor structures,⁹ for $\text{Al}_x\text{Ga}_{1-x}\text{As}/\text{GaAs}$ heterostructures,¹¹ and for $\text{In}_{1-x}\text{Ga}_x\text{As}$ quantum wells.²¹

The range of validity of Eq. (4) is the critical regime ($\epsilon \ll 1$). However, outside the critical regime the numerical differences between Eq. (4) and the numerical results within the formulation of the multiple-scattering theory as given in Refs. 9 and 17, and used in Refs. 9, 11, and 21 for the interpretation of some experimental results, are very small. Equation (4) can also be used if several scattering mechanisms $i = 1, 2, \dots, k$ are present:⁹ $A = A_1 + A_2 + \dots + A_k$ and $1/\sigma_0 = 1/\sigma_{01} + 1/\sigma_{02} + 1/\sigma_{0k}$.

In Fig. 1 I show the mobility μ versus electron density for remote impurity doping and homogeneous background doping (see later). The solid line represents Eq. (4) [$\mu(N) = \mu_0(N)(1 - A)$] and the dotted line represents $\mu_0(N)$. The dashed line represents the multiple-scattering theory in the formulation of Ref. 9.

The calculation of the conductivity is for zero tempera-

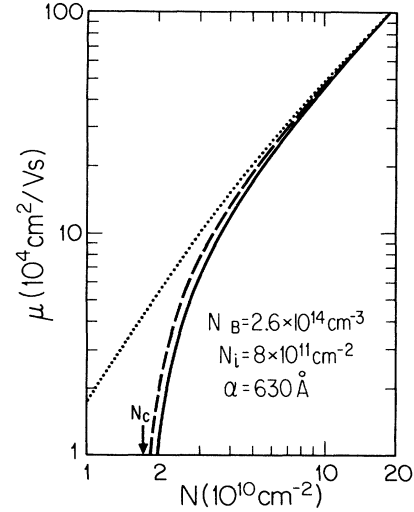


FIG. 1. Mobility vs electron density for remote impurity doping and homogeneous background doping. The dotted, dashed, and solid lines represent the Born approximation, the multiple-scattering theory in the formulation of Ref. 9, and Eq. (4), respectively. I used the following: width of remote doping $\delta = 350 \text{ \AA}$; depletion density $N_D = 1 \times 10^{11} \text{ cm}^{-2}$.

ture. The experiments must be performed at finite temperatures and a careful study of the temperature dependence of the conductivity is necessary to extrapolate to zero temperature (to eliminate the electron-phonon interaction).

C. The mean free path

The transport mean free path $l^{(t)}$ for $N = N_c$, calculated in Born approximation, is expressed as

$$k_{Fc} l_c^{(t)} = 2k_{Fc} \alpha \gg 1. \quad (12)$$

This result is in agreement with the estimate of Efros:¹² $k_{Fc} l \sim (N_i \alpha^2)^{1/4}$. With $N_i \approx \alpha^2 k_{Fc}^4$ from Eq. (5) I find Eq. (12).

$l_c^{(t)} = 2\alpha$ is the Joffe-Regel criterion (originally formulated for three-dimensional systems;²⁴ for two-dimensional systems, see Ref. 16) for the lower limit of the transport mean free path for long-range random potentials. The transport mean free path (or the scattering time $\tau^{(t)}$) at the metal-insulator transition is large for large α . However, this does not imply that the amount of disorder in the systems is small. For long-range random potentials backscattering is sharply reduced and the scattering time is greatly enhanced.¹⁶

A better measure of the amount of disorder in the system is the single-particle mean free path $l^{(s)}$ (single-particle relaxation time $\tau^{(s)}$).²⁵ For large α the ratio is larger than one^{21,26} and given by $\tau^{(t)}/\tau^{(s)} = (2k_{Fc}\alpha)^2$ for $2k_{Fc}\alpha \gg 1$.²¹ It follows that at $N = N_c$

$$k_{Fc} l_c^{(s)} = 1/(2k_{Fc} \alpha) \ll 1. \quad (13a)$$

In this case multiple-scattering effects become important and the single-particle relaxation time is renormalized: $\tau^{(\text{sr})}$. Consequently one has a renormalized single-particle mean free path $l^{(\text{sr})}$: $k_F l^{(\text{sr})} = 2\varepsilon_F \tau^{(\text{sr})}$. ε_F is the Fermi energy. Multiple-scattering effects for the single-particle relaxation time have been calculated in Ref. 21. With Eq. (47) of Ref. 21 I get at the metal-insulator transition point

$$k_{Fc} l_c^{(\text{sr})} = \left(\frac{1}{2}\right)^{1/2} \quad (13b)$$

and

$$k_F l^{(\text{sr})} = 2\alpha k_F (g_v N / N_i)^{1/2} = 1/(2A)^{1/2}. \quad (13c)$$

For short-range potentials one finds $\tau^{(t)}/\tau^{(s)} \simeq 1$ (Ref. 25) and $l_c^{(s)} \simeq l_c^{(\text{sr})}$.²¹ The Joffe-Regel criterion is given as $k_{Fc} l_c^{(t)} \simeq k_{Fc} l_c^{(s)} \simeq k_{Fc} l_c^{(\text{sr})} \sim O(1)$. I conclude: $l_c^{(t)}$ is very different for long-range and short-range random potentials.^{16,24} However, for the renormalized single-particle mean free path I find for short-range and long-range random potentials

$$k_{Fc} l_c^{(\text{sr})} \simeq O(1). \quad (14)$$

This is an additional criterion for the metal-insulator transition based on the single-particle relaxation time. It does not depend on the range of the random potential. This result shows that for localization the amount of disorder as given in the single-particle relaxation time is important. For the transport mean free path the relation $k_F l^{(t)} \gg 1$ is not conclusive to argue for weak disorder. The correct relation for weak disorder is $k_F l^{(t)} \gg 2k_F \alpha$. This argument should be kept in mind in analyzing experiments.

D. Density of states

From Eq. (13c) I conclude, see Eq. (48) of Ref. 21, that the density of states (ρ_r) is renormalized (r) due to the random potential. At the metal-insulator transition I find $\rho_{rc} = 0.73\rho_F$. In the multiple-scattering approach for the conductivity^{9,11,14-17} effects of disorder on the polarization are neglected. For Eq. (5) I used $X^0(q) = \rho_F$.

One could ask whether the effects of disorder on the density of states would change the parameter A as given in Eq. (5). With $X^0(q) = \rho_r$ and $\varepsilon(q) = q_{sr}/q$ one can show that Eq. (5) is rederived if one applies $q_{sr} = 2\pi e^2 \rho_r / \varepsilon_L$. This result shows that disorder effects on the density of states do not play a role in the calculation of parameter A for long-range random potentials.

E. Doping considerations

For homogeneous background doping a similar calculation as done for remote doping gives the critical concentration¹⁴

$$N_c = \frac{N_B^{2/3}}{(2\pi g_v)^{1/3}} \quad (15)$$

and N_B is the (three-dimensional) impurity density. Scattering by homogeneous background doping has been identified in recent experiments on $\text{Al}_x\text{Ga}_{1-x}\text{As}/\text{GaAs}$

heterostructures.^{27,28} For $N_B = 1 \times 10^{14} \text{ cm}^{-3}$, as in experiment, I get $N_c = 1.2 \times 10^9 \text{ cm}^{-2}$. I conclude that for a study of the metal-insulator due to homogeneous background doping a high-doping level is necessary to reach the experimentally available density regime $N > 1 \times 10^{10} \text{ cm}^{-2}$. Equation (15) is important for an estimation of a possible interplay between remote doping and homogeneous background doping. It is clear from my discussion that the conductivity near the metal-insulator transition is determined by remote doping if $N_B \ll N_i / (128\pi g_v N \alpha^4)^{1/2}$.

If I assume that the doping region has a width δ [see Eq. (1) of Ref. 11] I get with Eq. (2b)

$$N_c = \frac{N_i^{1/2}}{4\pi^{1/2}\alpha} \left[\frac{1}{1+\delta/\alpha} \right]^{1/2}. \quad (16)$$

N_c is reduced for finite δ .

The results have been derived within the conditions $4k_F \alpha \gg 1$ and $4g_v \alpha / a^* \gg 1$. If I give up the latter condition [I use Eqs. (1) and (2a)] I get

$$A = -\frac{g_v^2 N_i}{\pi N N a^{*2}} [1 + e^{4g_v \alpha / a^*} \text{Ei}(-4g_v \alpha / a^*) \times (1 + 4g_v \alpha / a^*)] \quad (17)$$

and corrections to Eq. (6) can be derived. $\text{Ei}(x)$ is the exponential-integral function. The asymptotic result for $4g_v \alpha / a^* \gg 1$ is written as

$$N_c = \frac{N_i^{1/2}}{4\pi^{1/2}\alpha} \left[1 - \frac{a^*}{g_v \alpha} + \frac{9a^{*2}}{8g_v^2 \alpha^2} - O(\alpha^{-3}) \right]. \quad (18)$$

N_c is reduced in comparison to Eq. (6) because Eq. (2b) underestimates the screening properties of the electron gas. Equation (18) demonstrates the power of the multiple-scattering method: It is not limited by $4k_F \alpha \gg 1$ or $4g_v \alpha / a^* \gg 1$.

Doping in GaAs ($\alpha < 0$) has been considered in Ref. 29 and the critical electron concentration was calculated. In this case the finite extension of the electron gas perpendicular to the $\text{Al}_x\text{Ga}_{1-x}\text{As}/\text{GaAs}$ interface has to be taken into account. One finds $A \sim N_i f(\alpha) / N^2$ and $f(\alpha)$ is a nonmonotonic function of α .²⁹

Naively one would assume $N = N_i$ to ensure charge neutrality. N_c would be very small for large spacer width. I believe that two possibilities exist to increase N_c : $N_i \gg N_c$. The first possibility is to use a compensated doping layer with compensation K_0 . Then one finds

$$N_i = N \frac{1+K_0}{1-K_0} \quad (19)$$

and $N_i \gg N$ for $K_0 \simeq 1$. With Eqs. (6) and (19) I get

$$N_c = \frac{1}{16\pi\alpha^2} \frac{1+K_0}{1-K_0}. \quad (20)$$

For $\alpha = 500 \text{ \AA}$ ($\alpha = 5a^*$ for $\text{Al}_x\text{Ga}_{1-x}\text{As}/\text{GaAs}$ heterostructures) one gets $N_c = 8.0 \times 10^8 \text{ cm}^{-2}$ (for $K_0 = 0$), $N_c = 1.5 \times 10^{10} \text{ cm}^{-2}$ (for $K_0 = 0.9$), and $N_c = 1.6 \times 10^{11} \text{ cm}^{-2}$ (for $K_0 = 0.99$). The second possibility is a nearby

gate on top of $\text{Al}_x\text{Ga}_{1-x}\text{As}$. In this case most of the electrons from the donors will go to the gate and only a small fraction will be trapped in the potential well of the heterostructure ($N_i \gg N$). Such a structure was already used in experiments,⁶ see also Table I of Ref. 11.

Interface-roughness scattering is not expected to play an important role in heterostructures at low electron densities (where the metal-insulator transition occurs). At low electron densities the envelope wave function perpendicular to the $\text{Al}_x\text{Ga}_{1-x}\text{As}/\text{GaAs}$ interface is very extended and the interface-roughness scattering potential is small.⁷ However, in thin quantum wells the interface-roughness scattering might be much more important, as discussed in Ref. 14.

IV. COMPARISON WITH EXPERIMENTS

In the following I apply my theory to mobility measurements on $\text{Al}_x\text{Ga}_{1-x}\text{As}/\text{GaAs}$ heterostructures¹³ which are intentionally doped with two doping spikes. These samples are unique because of the large spacers, see Fig. 2. In previous samples with high mobility³⁻⁶ the mobility has been measured only in the "high" density range ($N > 2 \times 10^{10} \text{ cm}^{-2}$). Mobility measurements down to very low densities $N \approx 1 \times 10^9 \text{ cm}^{-2}$ (where multiple-scattering effects become important) are essential for the study of the MIT in heterostructures with large spacers.

In the experiments of Ref. 13 the mobility versus electron density was measured for samples with very large spacers at a very low temperature of 28 mK. The results of Ref. 13 are shown in Fig. 3. For sample M73 two doping spikes at $\alpha = 2800 \text{ \AA}$ ($N_i = 1.8 \times 10^{11} \text{ cm}^{-2}$) and $\alpha = 4200 \text{ \AA}$ ($N_i = 1.2 \times 10^{12} \text{ cm}^{-2}$) have been implanted into the $\text{Al}_x\text{Ga}_{1-x}\text{As}$, see Fig. 2 and Ref. 28. From the data for sample M73 I conclude that a MIT takes place at $N_c \sim 4 \times 10^9 \text{ cm}^{-2}$. The variation of the mobility with electron density for $N \gg N_c$ indicates that background doping is the relevant scattering mechanism.

If I assume that all the donors in the doping spikes are electrically active I get with Eq. (5) $A_R = 1.8 \times 10^{19} / N^2 \text{ cm}^4$ (R for remote doping) and with Eq. (8) $\mu_R = 2.4 \times 10^{-9} N^{3/2} \text{ cm}^5/\text{V s}$. The critical electron density for the MIT is $N_c = 4.3 \times 10^9 \text{ cm}^{-2}$, which is in rough agreement with the experimental result. The results of

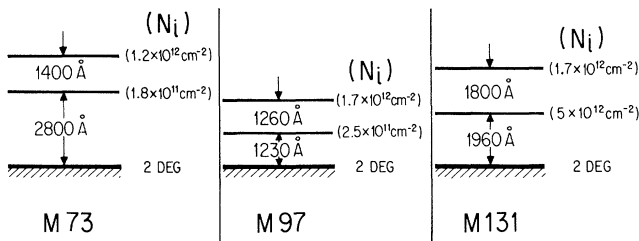


FIG. 2. Schematic picture of the doping profile for remote doping of the $\text{Al}_x\text{Ga}_{1-x}\text{As}/\text{GaAs}$ heterostructures M73, M97, and M131 of Ref. 13. For the doping profile of sample M73 see also Ref. 28.

my calculation for remote impurities and homogeneous background doping (for $N_B = 6 \times 10^{13} \text{ cm}^{-3}$) are shown in Fig. 3. I conclude that the MIT in sample M73 is due to remote doping while the conductivity scale at the MIT is determined by homogeneous background doping. An even better agreement between theory and experiment than shown in Fig. 3 could be obtained by reducing the impurity concentration by 10%. The MIT for homogeneous background doping (if no remote doping is present) is estimated to occur at $N_c \approx 8.3 \times 10^8 \text{ cm}^{-2}$ for $N_B = 6 \times 10^{13} \text{ cm}^{-3}$.

The two doping spikes (N_{i1}, N_{i2}) of sample M73 can be replaced by a single doping spike with $N_i = (N_{i1} + N_{i2})/2 = 6.9 \times 10^{11} \text{ cm}^{-2}$. I get the same value of N_c as for the two doping spikes if I choose $\alpha = 2760 \text{ \AA}$. The calculated mobility for $\alpha = 2760 \text{ \AA}$ and $N_i = 6.9 \times 10^{11} \text{ cm}^{-2}$ is very similar to the dotted line in Fig. 3. In Ref. 11 I have analyzed the experiments of Ref. 6 with $N_i = 6.0 \times 10^{11} \text{ cm}^{-2}$ and $350 < \alpha < 750 \text{ \AA}$. The experimental results of Refs. 6 and 13 confirm the spacer width dependence of N_c , see Eq. (6).

I would like to stress that only N_B was used as a fit parameter for the calculation of the solid line in Fig. 3. The homogeneous background doping must be considered as unintentional doping and is therefore not known from the growth process. The good agreement of the theoretical results with the experimental results of Ref. 13 supports the arguments that (i) a metal-insulator transition takes place in two-dimensional systems (possibly a transition from weakly localized states to strongly localized states) and (ii) that the critical electron density is determined by remote doping, see Eq. (6). The experimental results of Refs. 6 and 13 on the critical electron density depend on the width of the spacer and cover the range $4 \times 10^9 < N_c < 4 \times 10^{10} \text{ cm}^{-2}$.

For the depletion density I chose $N_D = 1 \times 10^{11} \text{ cm}^{-2}$.

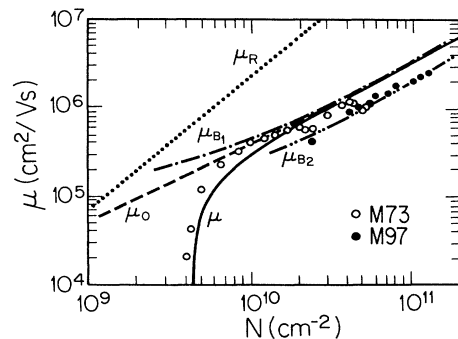


FIG. 3. Mobility vs electron density for remote doping (μ_R for a doping structure corresponding to M73) and for homogeneous background doping (μ_{B1} for $N_{B1} = 6 \times 10^{13} \text{ cm}^{-3}$ and μ_{B2} for $N_{B2} = 1 \times 10^{14} \text{ cm}^{-3}$) in Born approximation. The dashed line represents the mobility μ_0 for both scattering mechanisms (μ_R, μ_{B1}) in Born approximation. The solid line represents the mobility calculated within the multiple-scattering approach. The open and solid circles represent the experimental results of Ref. 13.

However, N_D does not enter the expressions for remote doping. The homogeneous background doping depends only weakly on N_D and a slightly different background doping density can account for this dependence.

The sample M97 (doping spikes: $\alpha=1230$ Å with $N_i=2.5 \times 10^{11} \text{ cm}^{-2}$ and $\alpha=2490$ Å with $N_i=1.7 \times 10^{12} \text{ cm}^{-2}$, see Fig. 2) apparently has a larger background doping density ($N_B=1 \times 10^{14} \text{ cm}^{-3}$) than sample M73, see Fig. 3. For sample M97 I get $A_R=9.4 \times 10^{19}/N^2 \text{ cm}^4$ and $\mu_R=2.5 \times 10^{-10} N^{3/2} \text{ cm}^5/\text{Vs}$ for the two doping spikes and the critical electron density for the MIT is predicted to occur at $N_c=9.4 \times 10^9 \text{ cm}^{-2}$.

The argument used above for the homogeneous background doping density of sample M97 did not include the remote impurities. Indeed, if the remote doping is also taken into account I conclude that the background doping density in sample M97 is the same as in sample M73. The theoretical results on the mobility of samples M93, M97, and M131 are shown in Fig. 4 for $N_B=6 \times 10^{13} \text{ cm}^{-3}$. The agreement between theoretical results and experimental results on sample M131 (doping spikes: $\alpha=1960$ Å with $N_i=5 \times 10^{12} \text{ cm}^{-2}$ and $\alpha=3760$ Å with $N_i=1.7 \times 10^{12} \text{ cm}^{-2}$, see Fig. 2) is very good. The MIT in sample M131 is predicted to occur at an electron density $N_c=1.8 \times 10^{10} \text{ cm}^{-2}$ ($A_R=2.8 \times 10^{20}/N^2 \text{ cm}^4$, $\mu_R=8.7 \times 10^{-11} N^{3/2} \text{ cm}^5/\text{Vs}$). A study of the behavior of the mobility of samples M97 and M131 at low electron density would be highly desirable, see Fig. 4.

Comparing in Fig. 4 the dashed lines (μ_0) with the dotted lines (μ_B) lead us to the conclusion that for samples M97 and M131 the remote doping contributes to the scattering time even at the highest measured electron density ($N \approx 1 \times 10^{11} \text{ cm}^{-2}$). This is not the case for sample M73, see Fig. 3. In sample M131 the MIT and the mobility scale at the MIT are determined by the remote impurity doping. In sample M97 both scattering mechanisms contribute to the mobility scale at the MIT.

I would like to mention that the sample of Ref. 5 with ultrahigh mobility ($\mu=1.1 \times 10^7 \text{ cm}^2/\text{Vs}$) had a single doping spike with $\alpha=700$ Å ($N_i=1 \times 10^{12} \text{ cm}^{-2}$) and I

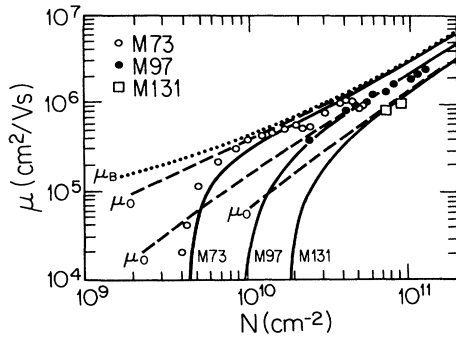


FIG. 4. Mobility μ and μ_0 (see Fig. 3) for remote doping (for doping structures corresponding to M73, M97, and M131) and homogeneous background doping (μ_B for $N_B=6 \times 10^{13} \text{ cm}^{-3}$). The open circles, solid circles, and the open squares represent the experimental results of Ref. 13.

expect the MIT at $N_c=2 \times 10^{10} \text{ cm}^{-2}$. Unfortunately, for this sample only the mobility data for $N \geq 1.5 \times 10^{11} \text{ cm}^{-2}$ has been reported. For the sample with $\alpha=2000$ Å (Ref. 5) I get $N_c=7 \times 10^9 \text{ cm}^{-2}$ if I assume $N_i=1 \times 10^{12} \text{ cm}^{-2}$. The mobility was reported for $N > 2 \times 10^{10} \text{ cm}^{-2}$. The theoretical estimates for N_c are not in contradiction with the published data of Ref. 5.

However, I have to admit that the mobility of the sample⁵ with $\alpha=700$ Å ($N_i=1 \times 10^{12} \text{ cm}^{-2}$) cannot be explained by the doping structure. For $N=2 \times 10^{11} \text{ cm}^{-2}$ I get $\mu_R=1.9 \times 10^6 \text{ cm}^2/\text{Vs}$ while the experiment gives $\mu \sim 1.1 \times 10^7 \text{ cm}^2/\text{Vs}$. I conclude that the origin of the unexpected high mobility of this sample is presently not understood. A possible explanation is that the doping spike is electrically not active and the donors in the doping spike are neutral. Moreover, the density dependence of the mobility of the samples studied in Ref. 5 suggests that the mobility is limited by homogeneous background doping.³⁰

V. DISCUSSION

The comparison between theoretical and experimental results on the mobility of $\text{Al}_x\text{Ga}_{1-x}\text{As}/\text{GaAs}$ heterostructures indicates that the transport properties of two-dimensional electron systems are well described by a MIT. This result is in contradiction with the theoretical claim of the absence of a metallic phase in two dimension at temperature zero.¹ Within the scaling theory one would probably argue that for very low temperatures the apparently metallic systems would eventually become insulating. It should be noted that the scaling theory¹ has been derived for a noninteracting electron gas with short-range disorder. However, the random potential for remote doping is a long-range random potential. In Ref. 31 it has been shown that for a long-range random potential the scattering time is very strongly frequency dependent due to plasmon dynamics.

I argue that in experiments, which are always performed at a finite temperature, the transport properties of the studied two-dimensional systems are apparently determined by the scattering mechanisms ($\mu \propto N^\gamma$) and the strength of the disorder ($A \ll 1$ or $A \sim 1$) and not so much determined by the temperature of the sample. After measuring the mobility of a sample at say 1 K a mobility measurement at 0.1 K will nearly give the same number (up to some percents²). However, if the electron density near $A \approx 1$ is changed by 10% the mobility changes are dramatic, see Figs. 1, 3, and 4.

The percolation picture proposed by Efros¹² gives a critical electron density similar to my result: $N_c \propto N_i^{1/2}/\alpha$. However, it is not so clear how to calculate the mobility for remote doping in the percolation picture for $N > 1.1N_c$. Scaling laws near the transition presumably are only valid near N_c ($N < 1.1N_c$) and provide no predictions for $N > 1.1N_c$. It would be very interesting to study the MIT when only homogeneous background doping is important. These measurements could supply a strong argument for the relevance of the multiple-scattering theory because no predictions has been made for this scattering mechanism within the percolation ap-

proach.

After measuring the mobility of a sample at low temperatures the experimenter would like to know whether the measured mobility corresponds to the doping profile (assuming that the donors are electrically active). Mobility calculations in lowest order cannot describe the experimental results at low electron densities where $A \approx 1$. The mobility μ_0 and the parameter A depend on the range of the random potential (short-range or long-range random potential). The knowledge of the scattering mechanism and the range of the random potential is necessary to compare other experimental results (as, for example, the cyclotron line width⁷) with theoretical predictions. My results strongly suggest that the transport properties of the two-dimensional electron gas in $\text{Al}_x\text{Ga}_{1-x}\text{As}/\text{GaAs}$ heterostructures can be described by the scattering mechanisms and the parameter A .

If the percolation picture is correct one would expect that the logarithmic temperature dependence of the conductivity, which is characteristic for weak-localization effects,¹ is absent. Only the logarithmic temperature dependence of the conductivity due to interaction effects³² eventually remains.

In the theory I have neglected the possible formation of impurity bands. In the presence of impurity bands my analysis as well as the scaling theory¹ is not applicable. For large α and for high impurity concentration a band-tail description is possible³³ and my theory should be valid.

VI. CONCLUSION

In conclusion I have shown that the multiple-scattering approach for the conductivity, which has been used for some time for the interpretation of experiments on transport anomalies in two-dimensional systems,^{9,11,21} gives (for remote doping) similar results as the percolation approach recently proposed by Efros.¹² The relation between the scattering time and the single-particle relaxation time at the metal-insulator transition has been discussed. The analytical results should be helpful in designing crucial experiments for the study of the metal-insulator transition in two-dimensional systems.

My analytical results successfully describe mobility measurements on samples¹³ with low mobilities (at low electron densities) and with high mobilities (at high electron densities). More experiments on similar $\text{Al}_x\text{Ga}_{1-x}\text{As}/\text{GaAs}$ heterostructures with smaller spacers ($\alpha < 300 \text{ \AA}$) would be very helpful for a better understanding of the transport anomalies in these structures.

ACKNOWLEDGMENTS

I am grateful to P. A. Lee and M. Shayegan for stimulating discussions. This work was supported by the Deutsche Forschungsgemeinschaft (Bonn, Germany) and the Joint Services Electronics Program (Contract No. DAAL03-89-C-0001).

*Present address: Laboratoire de Physique des Solides, Université Paul Sabatier, 118 Route de Narbonne, 31062 Toulouse, France.

¹E. Abrahams, P. W. Anderson, D. C. Licciardello, and T. V. Ramakrishnan, *Phys. Rev. Lett.* **42**, 673 (1979).

²P. A. Lee and T. V. Ramakrishnan, *Rev. Mod. Phys.* **57**, 287 (1985).

³J. H. English, A. C. Gossard, H. L. Störmer, and K. W. Baldwin, *Appl. Phys. Lett.* **50**, 1826 (1987).

⁴C. T. Foxon, J. J. Harris, D. Hilton, J. Hewett, and C. Roberts, *Semicond. Sci. Technol.* **4**, 582 (1989).

⁵L. Pfeiffer, K. W. West, H. L. Stormer, and K. W. Baldwin, *Appl. Phys. Lett.* **55**, 1888 (1989).

⁶C. Jiang, D. C. Tsui, and G. Weimann, *Appl. Phys. Lett.* **53**, 1533 (1988).

⁷T. Ando, A. B. Fowler, and F. Stern, *Rev. Mod. Phys.* **54**, 437 (1982).

⁸D. A. Anderson, S. J. Bass, M. J. Kane, and L. L. Taylor, *Appl. Phys. Lett.* **49**, 1360 (1986).

⁹A. Gold and W. Götze, *Solid State Commun.* **47**, 627 (1983); *Phys. Rev. B* **33**, 2495 (1986). For comparison with experiments, see A. Gold, *Phys. Rev. Lett.* **54**, 1079 (1985); *Phys. Rev. B* **32**, 4014 (1985); *Surf. Sci.* **170**, 381 (1986); *Z. Phys. B* **63**, 1 (1986).

¹⁰J. J. Harris, J. A. Pals, and R. Woltjers, *Rep. Prog. Phys.* **52**, 1217 (1989).

¹¹A. Gold, *Appl. Phys. Lett.* **54**, 2100 (1989).

¹²A. L. Efros, *Solid State Commun.* **70**, 253 (1989).

¹³T. Sajoto, Y. W. Suen, L. W. Engel, M. B. Santos, and M. Shayegan, *Phys. Rev. B* **41**, 8449 (1990).

¹⁴A. Gold, *Solid State Commun.* **60**, 531 (1986).

¹⁵W. Götze, *Solid State Commun.* **27**, 1393 (1978).

¹⁶A. Gold and W. Götze, *J. Phys. C* **14**, 4049 (1981).

¹⁷A. Gold, Ph.D. thesis, Technical University, Munich, 1984.

¹⁸D. Vollhardt and P. Wölffe, *Phys. Rev. B* **22**, 4666 (1980).

¹⁹D. Belitz, A. Gold, and W. Götze, *Z. Phys. B* **44**, 273 (1981).

²⁰P. J. Price, *J. Vac. Sci. Technol.* **19**, 599 (1981).

²¹A. Gold, *Phys. Rev. B* **38**, 10 798 (1988).

²²B. I. Shklovskii and A. L. Efros, *Electronic Properties of Doped Semiconductors* (Springer, Berlin, 1984), Chap. 5.

²³B. I. Shklovskii and A. L. Efros, in *Electronic Properties of Doped Semiconductors* (Ref. 22), Chap. 13 (and other chapters).

²⁴A. F. Ioffe and A. R. Regel, *Prog. Semicond.* **4**, 237 (1960).

²⁵A. A. Abrikosov, L. P. Gorkov, and I. E. Dzyaloshinski, *Methods of Quantum Field Theory* (Prentice-Hall, Englewood Cliffs, NJ, 1963), Sec. 39.

²⁶J. P. Harrang, R. J. Higgins, R. K. Goodall, P. R. Jay, M. Laviron, and P. Delescluse, *Phys. Rev. B* **32**, 8126 (1985). See also S. Das Sarma and F. Stern, *ibid.* **32**, 8442 (1985).

²⁷M. Shayegan, V. J. Goldman, C. Jiang, T. Sajoto, and M. Santos, *Appl. Phys. Lett.* **52**, 1086 (1988).

²⁸M. Shayegan, V. J. Goldman, M. Santos, T. Sajoto, L. Engel, and D. C. Tsui, *Appl. Phys. Lett.* **53**, 2080 (1988).

²⁹A. Gold, *J. Phys. (Paris) Colloq.* **48**, C5-255 (1987).

³⁰A. Gold, *Phys. Rev. B* **41**, 8537 (1990).

³¹A. Gold, *Phys. Rev. B* **41**, 3608 (1990).

³²B. L. Altshuler, A. G. Aronov, and P. A. Lee, *Phys. Rev. Lett.* **44**, 1288 (1980).

³³J. Serre, A. Ghazali, and A. Gold, *Phys. Rev. B* **39**, 8499 (1989).